

MyD88 Signaling Pathway Is Involved in Renal Fibrosis by Favoring a T_H2 Immune Response and Activating Alternative M2 Macrophages

Tarcio Teodoro Braga,¹ Matheus Correa-Costa,¹ Yuri Felipe Souza Guise,¹ Angela Castoldi,² Cassiano Donizetti de Oliveira,² Meire Ioshie Hyane,¹ Marcos Antonio Cenedeze,² Simone Aparecida Teixeira,³ Marcelo Nicolas Muscara,³ Katia Regina Perez,⁴ Iolanda Midea Cuccovia,⁴ Alvaro Pacheco-Silva,² Giselle Martins Gonçalves,¹ and Niels Olsen Saraiva Camara^{1,2}

¹Laboratory of Transplantation Immunobiology, Department of Immunology, Institute of Biomedical Sciences IV, University of São Paulo (USP), São Paulo, Brazil; ²Laboratory of Clinical and Experimental Immunology, Nephrology Division, Federal University of São Paulo (UNIFESP), São Paulo, Brazil; ³Department of Pharmacology, Institute of Biomedical Sciences; and ⁴Department of Biochemistry, Institute of Chemistry, University of São Paulo (USP), São Paulo, Brazil

Inflammation contributes to the pathogenesis of chronic kidney disease (CKD). Molecules released by the inflamed injured tissue can activate toll-like receptors (TLRs), thereby modulating macrophage and CD4⁺ T-cell activity. We propose that in renal fibrogenesis, M2 macrophages are recruited and activated in a T helper subset 2 cell (T_H2)-prone inflammatory milieu in a MyD88-dependent manner. Mice submitted to unilateral ureteral ligation (UUO) demonstrated an increase in macrophage infiltration with collagen deposition after 7 d. Conversely, TLR2, TLR4 and MyD88 knockout (KO) mice had an improved renal function together with diminished T_H2 cytokine production and decreased fibrosis formation. Moreover, TLR2, TLR4 and MyD88 KO animals exhibited less M2 macrophage infiltration, namely interleukin (IL)-10⁺ and CD206⁺ CD11b^{high} cells, at 7 d after surgery. We evaluated the role of a T_H2 cytokine in this context, and observed that the absence of IL-4 was associated with better renal function, decreased IL-13 and TGF-β levels, reduced arginase activity and a decrease in fibrosis formation when compared with IL-12 KO and wild-type (WT) animals. Indeed, the better renal outcomes and the decreased fibrosis formation were restricted to the deficiency of IL-4 in the hematopoietic compartment. Finally, macrophage depletion, rather than the absence of T cells, led to reduced lesions of the glomerular filtration barrier and decreased collagen deposition. These results provide evidence that future therapeutic strategies against renal fibrosis should be accompanied by the modulation of the M1:M2 and T_H1:T_H2 balance, as T_H2 and M2 cells are predictive of fibrosis toward mechanisms that are sensed by innate immune response and triggered in a MyD88-dependent pathway.

Online address: <http://www.molmed.org>

doi: 10.2119/molmed.2012.00131

INTRODUCTION

Chronic kidney disease (CKD) is a major health problem, highly prevalent in the general population, and associated with a high mortality rate mainly due to cardiovascular complications (1). Several animal models have been used to study

different features of CKD (2), and the use of genetically engineered mice has greatly expanded the utility of this model in studying molecular mechanisms underlying the renal response to chronic insults (3). Specifically, unilateral ureteral ligation (UUO) induces, after a

few hours, cellular infiltration into the kidney, mainly macrophages that secrete growth factors and cytokines that ultimately induce disequilibrium between apoptosis and proliferation of the tubular cells, which favors fibroblast activation and proliferation. Activated fibroblasts secrete additional extracellular matrix (ECM) components that accumulate in the interstitium, and, as the obstruction continues, ECM deposition becomes massive, and the uncontrolled apoptosis of cells results in tubular atrophy (3). This matrix remodeling and cellular stress can release molecules that finally instigate an inflammatory response.

Toll-like receptors (TLRs) are an innate family of receptors that can sense tissue

Address correspondence to Niels Olsen Saraiva Câmara, Department of Immunology, Institute of Biomedical Sciences, University of São Paulo, Cidade Universitária, Av. Prof. Lineu Prestes, 1730, 05508-900, São Paulo, Brazil. Phone: +55-11-3091-7388; Fax: +55-11-3091-7224; E-mail: niels@icb.usp.br.

Submitted March 21, 2012; Accepted for publication July 5 2012; Epub (www.molmed.org) ahead of print July 5, 2012.

damage and orchestrate a cascade of inflammation following obstruction. Recent reports have shown reduced fibrosis in TLR4-deficient mice in a renal (4) and a hepatic (5) model of fibrotic diseases. In addition, the obstructed kidneys of TLR2-deficient mice demonstrated a decrease in the number of interstitial myofibroblasts in the later phase of nephropathy, even with no differences in collagen deposition (6). TLR2 and TLR4 signal via the intracellular adaptor molecule MyD88, although only a few studies implicated a role for MyD88 in fibrosis (7). TLRs modulate the immune system through the production of different cytokines, and influence the differentiation of immune cells. In a lung model of chronic disease, adaptive T_H2 cell immunity is essential to the promotion of fibrosis (8,9). In fact, cytokines are related to the adaptive immune response outcome in chronic inflammatory diseases, whereas fibrosis is strongly linked to the development of a T_H2-biased response (involving interleukin [IL]-4, IL-5 and IL-13) (10–12).

Macrophages are considered to play a pivotal role in the development of renal fibrosis (13,14). Recent studies raise the possibility that the effector phenotype of the recruited macrophages, rather than their presence, determines the extent of renal parenchymal injury (15,16). Macrophages are classified in distinct subpopulations according to their response to innate or adaptive immune signals. The term “classically activated” has been used to designate the effector macrophages that are produced during cell-mediated immune responses (17). Such macrophages also are designated M1 macrophages and express iNOS, CXCL9, CCR7, CXCL11, IL-12 and interferon (IFN)- γ . On the other hand, one of the first innate signals released during tissue injury is thought to be IL-4, an inducer of “alternatively activated” or M2 macrophages (18). Basophils and mast cells are important early sources of innate IL-4 production, although other granulocytes also might contribute (19). Besides IL-4, IL-13 can induce arginase-1 and collagen

deposition (19,20). Imbalance in production and catabolism of collagen, associated with prolonged IL-13 effects on macrophages, promotes excessive fibrosis. M2 macrophages express CD206, IL-10, arginase-1, FIZZ-1, YM-1 and RELM- α . One aspect to be elucidated is to what extent T_H2 cytokines and M2 macrophages contribute to noninfectious causes of fibrosis.

Since collagen deposition is a hallmark of all chronic diseases, preceded by the development of sterile inflammation which can be modulated by the presence of cytokines, here, we postulated that MyD88-dependent pathways could be involved in sensing these tissue alterations and in favoring a T_H2-prone profibrotic immune response.

MATERIALS AND METHODS

Animal Studies

Male TLR2, TLR4, MyD88, IL-4, IL-12 and Rag-1 knockout (KO) mice in H-2^b background and control C57Bl/6, aged 6 to 8 wks, were bred and housed in a pathogen-free facility. They were kept on a 12 h light:dark cycle in a temperature-controlled room at 21–23°C, with free access to water and food. Mice were anesthetized with ketamine–xylazine (Agribands do Brazil, Sao Paulo, Brazil). On d 0, UUO was performed by complete ligation of the right ureter. For each group, in a set of experiments, five mice were subjected to UUO and five used as sham mice. All procedures were approved by the internal ethical committee of the University of Sao Paulo (no. 45/2009).

Renal Function Outcomes

Urinary protein:creatinine ratio was measured in samples collected from the obstructed pelvis and from the bladder at 7 d after surgery. All samples were analyzed by colorimetric assays using commercially purchased kits for creatinine and protein measurements (Labtest, Minas Gerais, Brazil). The ratio was normalized dividing the ratio at d 7 by the ratio before surgery in each group of animals.

Fibrosis Quantification

Kidneys were collected in 10% buffered formaldehyde for fixation. Summarily, the slides were deparaffinized, rehydrated and immersed in saturated picric acid solution for 15 min and then in picosirius for 20 more minutes. Counterstaining was carried out with Harris hematoxylin. Picosirius-stained sections were analyzed by an Olympus BX50 microscope with an Olympus camera attached. Manual shots were taken of the cortex, magnified 40 \times , and observed under polarized light. Photos of at least 10 different fields in each slide were taken, and structures such as the glomeruli, subcapsular cortex, large vessels and medulla were excluded. For the morphometric analysis, the Image Processing and Analysis portion in ImageJ software (NIH, Bethesda, MD, USA; <http://rsbweb.nih.gov/ij/>) was used. The result of the analysis was represented by percentage, and refers to the proportion of the volume to the total cortical interstitial volume.

Immunohistochemistry

Immunohistochemistry was performed using a microwave-based antigen retrieval technique. Previously, the slides were deparaffinized, rehydrated and submitted to Tris-EDTA, pH 9, antigen retrieval solution at 95°C. The endogenous peroxidase activity was blocked with 3% hydrogen peroxide, and Protein Block Solution (DAKO, Glostrup, Denmark) was added. The slides were incubated with type I collagen (diluted 1:300; Abcam, Cambridge, MA, USA) and FSP-1 (diluted 1:600; A5114; DAKO, Ely, UK) antibodies or a negative control reagent, followed by incubation with the labeled polymer (Dual Link System-HRP; DAKO, Glostrup, Denmark) using two sequential 30-min incubations at room temperature. Staining was completed by performing a 1- to 3-min incubation with 3,3'-diaminobenzidine substrate-chromogen, which results in a brown-colored precipitate at the antigen site. Hematoxylin counterstaining was performed.

Hydroxyproline Quantification

Aliquots of standard hydroxyproline (Sigma, St. Louis, MO, USA) or kidney samples were hydrolyzed in alkali. The hydrolyzed samples then were mixed with a buffered chloramines-T reagent, and the oxidation was allowed to proceed for 25 min at room temperature. The chromophore then was developed with the addition of Ehrlich reagent and the absorbance of reddish purple complex was measured at 550 nm using a spectrophotometer. Absorbance values were plotted against the concentration of standard hydroxyproline, and the presence of hydroxyproline was determined using the standard curve (21).

Quantitative Real-Time

Total RNA was isolated from frozen kidney tissue using the TRIzol Reagent (Invitrogen; Life Technologies, Carlsbad, CA, USA) and protocol according to Invitrogen. RNA concentrations were determined by spectrophotometer readings at absorbance 260 nm. First-strand cDNAs were synthesized using the MML-V reverse transcriptase (Promega, Madison, WI, USA). Real-time polymerase chain reaction (RT-PCR) was performed using the TaqMan real-time PCR assay (Applied Biosystems, Life Technologies) for the following molecules: HPRT (Mm01545399_m1), tumor necrosis factor (TNF)- α (Mm00443258_m1), TLR2 (Mm00442346_m1), TLR4 (Mm00445273_m1), MyD88 (Mm00440338_m1), GATA-3 (Mm01337569_m1), TBX21 (Mm00450960_m1), type 1 collagen (Mm00801666_g1), IL-4 (Mm00445259_m1), arginase 1 (Mm01190441_g1), TSLP (Mm00498739_m1), iNOS (Mm00440485_m1) and TGF- β (Mm03024053_m1). Cycling conditions were as follows: 10 min at 95°C followed by 45 cycles at 20 s each at 95°C, 20 s at 58°C, and 20 s at 72°C. Analysis used Sequence Detection System (SDS) software version 1.9.1 Applied Biosystems, Life Technologies). mRNA expression was normalized to HPRT expression.

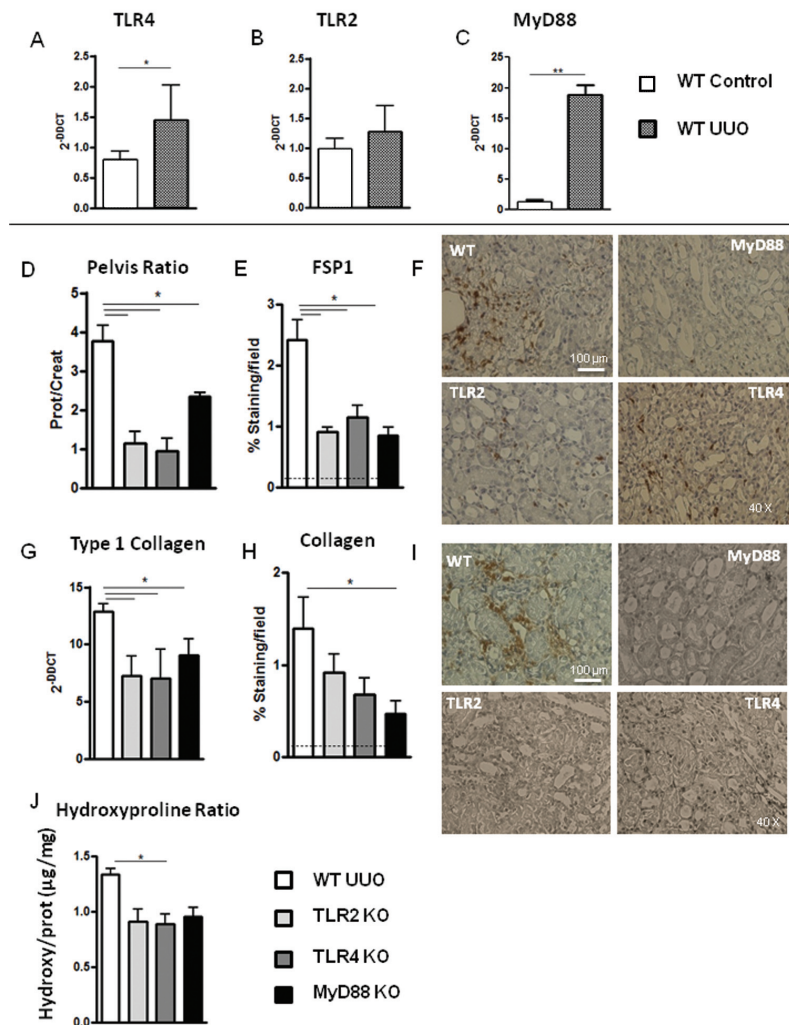


Figure 1. MyD88, TLR2 and TLR4 and renal fibrosis. TLR4 (A), TLR2 (B) and MyD88 (C) mRNA were quantified 7 d after surgery and compared to control animals nonsubmitted to UO. Pelvis proteinuria:creatininuria ratio (D) in all KO and in WT mice 7 d after UO. FSP-1 staining (E and F) and type-1 collagen mRNA (G) and staining (H and I) at 7 d after surgery in WT, TLR2, TLR4 and MyD88 KO animals. Renal tissue hydroxyproline ratio (J) in WT, TLR2, TLR4 and MyD88 KO animals. Immunohistochemistry is represented by the proportion of the staining area to the total area of the field. qPCR was normalized to HPRT, and the mean of WT control mice was considered 1. Dashed line represents WT animals not submitted to UO. * $p < 0.05$, ** $p < 0.01$.

Flow Cytometry

Infiltrating cells were analyzed by multicolor flow cytometry. The monoclonal antibodies used were F4/80 PerCP, CD11b PE, CD206 FITC, MIG PE, IL-10 APC, p40 (IL-12/IL-23) PE, CD4 Pacific Blue, IL-4 PerCP, IFN- γ FITC (all purchased from BD Biosciences, Franklin Lakes, NJ, USA). Samples were acquired on a FACSCanto, using

FACSDiva software (BD Biosciences) and then were analyzed with FlowJo software (Tree Star, Ashland, OR, USA). Fluorescence voltages were determined using matched unstained cells. Two hundred thousand events were acquired in a live mononuclear gate, and the compensation process was made according to the “fluorescence minus one” method.

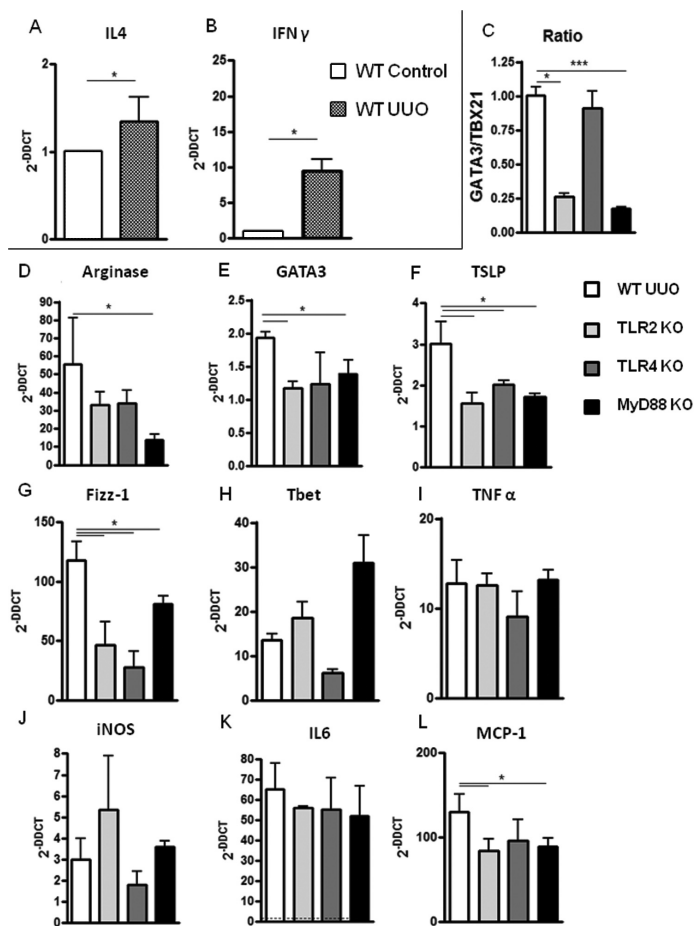


Figure 2. T_H2 pattern in WT, TLR2, TLR4 and MyD88 KO animals after UOU. UOU led to increased levels of IL-4 (A) and IFN- γ (B) mRNA in WT mice when compared to control animals. Renal GATA3:TBX21 ratio (C) in TLR2, TLR4, and MyD88 KO mice. The ratio of WT mice subjected to UOU was considered 1. Type 1 arginase (D), GATA-3 (E), TSLP (F), Fizz-1 (G), TBX21 (H), TNF α (I), iNOS (J), IL-6 (K), CD68 (L) and MCP1 (M) mRNA expression in kidneys in WT, TLR2, TLR4 and MyD88 KO animals 7 d after UOU. qPCR was normalized to HPRT, and the mean of the WT control mice was considered 1. * $p < 0.05$, ** $p < 0.01$.

Cytokines Determination by Enzyme-Linked Immunosorbent Assay

Tissue protein lysates were prepared by weighing frozen tissue and placing the samples in an appropriate amount of lysis buffer with protease inhibitors. Protein concentrations were determined using the Bradford protein assay (Thermo Scientific, Rockford, IL, USA). Total renal IL-13 (eBioscience, San Diego, CA, USA) and TGF β 1 (TGF β 1 Emax ImmunoAssay Systems, Promega) protein was measured according to the manufacturer's instructions. The results are presented as pg cytokine/mg of

total protein measured using the Bradford assay (Bio-Rad, Hercules, CA, USA).

Arginase Activity

The kidney samples were homogenized in lysis buffer and centrifuged for 30 min at 14000g at 4°C. Briefly, samples lysates were incubated with 10 mmol/L MnCl₂ and 50 mmol/L Tris-HCl (pH 7.5). The hydrolysis reaction of L-arginine by arginase was performed by incubating the mixture containing activated arginase and was stopped by adding acid solution. For calorimetric

determination of urea, α -isonitrosopropiophenone was added, and the mixture was heated at 100°C for 45 min. After placing the sample in the dark for 10 min at room temperature, the urea concentration was determined spectrophotometrically by the absorbance at 550 nm.

Liposome Preparation and Macrophage Depletion

Chlodronate (Bonafos, Schering, São Paulo, Brazil) was entrapped in liposomes by ether injection as described previously (22). Typically, 0.5 mL of an ether solution containing 50 mg phosphatidylcholine, and 8 mg cholesterol was injected (0.2 mL/minute) into 5 mL of a 50 mmol/L chlodronate aqueous solution maintained at 42°C. The liposome suspension was centrifuged at 22800g for 30 min (Hitachi Himac CR20B2 centrifuge, Hitachi, Troy, MI, USA) at 25°C. The liposome-containing pellet was washed twice by centrifugation under the same conditions in NaCl solution 0.9% (w/v). The final pellet was resuspended in 2 mL of saline solution. Typically, the final phosphatidylcholine and chlodronate concentrations in the liposomes were 10 mmol/L and 0.5 mmol/L, respectively. The yield of entrapped chlodronate was about 1% of the initial quantity added. Mice were injected intraperitoneally (IP) with 100 μ L of liposome preparation (6 μ g of chlodronate) 24 h before the UOU surgery. In addition, 200 μ L of liposome preparation (12 μ g of chlodronate), were administered IP during surgery and 3 d later.

Generation of BM Chimeric Mice

Male 6- to 8-wk-old IL-4 and IL-12 knockout (KO) mice were irradiated (11 Gy total body irradiation during 1,597 s). One h later, mice were reconstituted with 5×10^6 bone marrow (BM) cells from either IL-12 or IL-4 KO male donors. For the first 2 wks after BM transplantation, mice received 0.2% ciprofloxacin (Cipronil; Farmabase, Jaguariuna, Brazil) in their drinking

water. UUO was performed at 6 wks after the engraftment recovery period to allow full reconstitution of BM cells to occur.

Statistics

The data were described as mean and standard error of the mean (SEM). Differences among groups were compared using analysis of variance (ANOVA) (with Tukey *post hoc* test) and Student *t* test. Significant differences were regarded as $P < 0.05$. All statistical analyses were performed with the aid of GraphPad PRISM (GraphPad Software Inc., La Jolla, CA, USA).

All supplementary materials are available online at www.molmed.org.

RESULTS

TLR2, TLR4 and MyD88 are Involved in Renal Fibrogenesis

Sterile inflammation and cell death are present during remodeling of ECM in experimental models of CKD. Interestingly, such processes can release molecules that ultimately could be recognized by innate immune receptors in infiltrating cells and throughout the nephron (23). Thus, we initially investigated the expression of TLR2, TLR4 and MyD88 molecules in wild-type (WT) mice subjected to urine flow obstruction (Figures 1A–C). Since we observed an enhanced expression of those innate immune receptors, we next questioned whether they could be involved in renal disease progression. When subjected to UUO, all animals demonstrated a reduced proteinuria (Figure 1D), less deposition, protein and mRNA expression of type 1 collagen and lower infiltration of FSP1-positive cells as compared with WT mice (Figure 1E–I). UUO also enhances hydroxyproline quantity, the main amino acid that constitutes collagen (24). In this sense, TLR2, TLR4 and MyD88 KO mice presented decreased hydroxyproline rate (Figure 1J) compared with the WT mice. Altogether, our data demonstrate that TLRs participate in renal fibrosis.

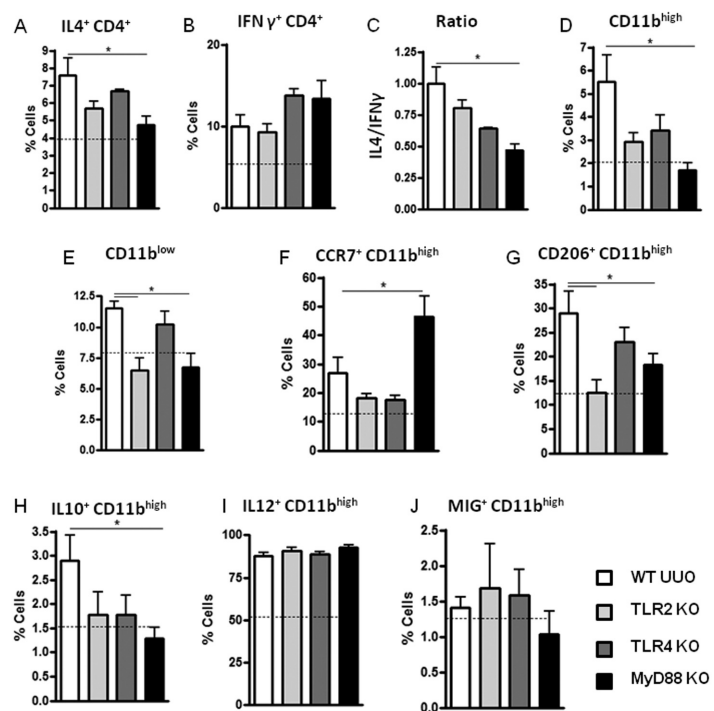


Figure 3. M2 immune response after UUO in WT, TLR2, TLR4 and MyD88 KO animals. Percentage of T CD4⁺ cells expressing IL-4 (A) and IFN- γ (B) in WT, TLR2, TLR4 and MyD88 KO animals 7 d after UUO. IL-4:IFN- γ ratio in TLR2, TLR4, and MyD88 KO mice (C). The ratio of WT mice subjected to UUO was considered 1. Percentage of infiltrating CD11b^{high} (D) and CD11b^{low} cells (E) and percentage of CD11b^{high} cells expressing CCR7(F), CD206(G), IL-10(H), IL-12 (p40) (I) and MIG (J) in WT, TLR2, TLR4 and MyD88 KO animals 7 d after UUO. Dashed line represents WT animals not submitted to UUO. * $p < 0.05$.

MyD88 Signaling Favors a T_H2 Pattern after UUO

Past studies have associated TLRs with the T_H2 immune response. In a pulmonary model of chronic disease, TLR4 polarized toward a T_H2 response by modulating dendritic cells (DCs) in both hematopoietic and stromal compartments (25). Thus, using our UUO model, we investigated whether the MyD88 pathway was involved in renal fibrosis by favoring a T_H2-biased response. As shown in Figures 2A and 2B, UUO led to increased mRNA levels of IL-4 and IFN- γ . Thus, we examined the GATA3:Tbet ratio. Indeed, this ratio was lower in TLR2 and MyD88 KO mice. Additionally, arginase-1, GATA3, TSLP and Fizz-1 mRNA, all T_H2 pattern-related molecules, were downregulated in MyD88 KO mice (Figures 2D–G). However, there were no differences in TBX21, TNF- α , iNOS and IL-6 mRNA in

TLR2, TLR4 and MyD88 KO compared with WT mice (Figures 2H–K). We also investigated MCP-1 mRNA in such animals, as shown in Figure 2L. TLR2- and MyD88-deficient animals present decreased expression of MCP-1 mRNA when compared with WT mice.

To confirm these results, we evaluated the percentage of kidney-infiltrating cells expressing T_H1:T_H2- and M1:M2-related molecules in those animals. The gate strategy to analyze cells is showed in Supplementary Figure S1. As expected, MyD88 KO mice showed a decreased percentage of IL-4⁺CD4⁺ cells (Figure 3A). However, the percentage of IFN- γ ⁺CD4⁺ did not change among all KO animals when compared with WT mice (Figure 3B). Then, we examined the IL-4/IFN- γ ratio, and we observed that MyD88 KO mice have the lowest ratio (Figure 3C). Considering the infiltration of myeloid cells, MyD88 KO

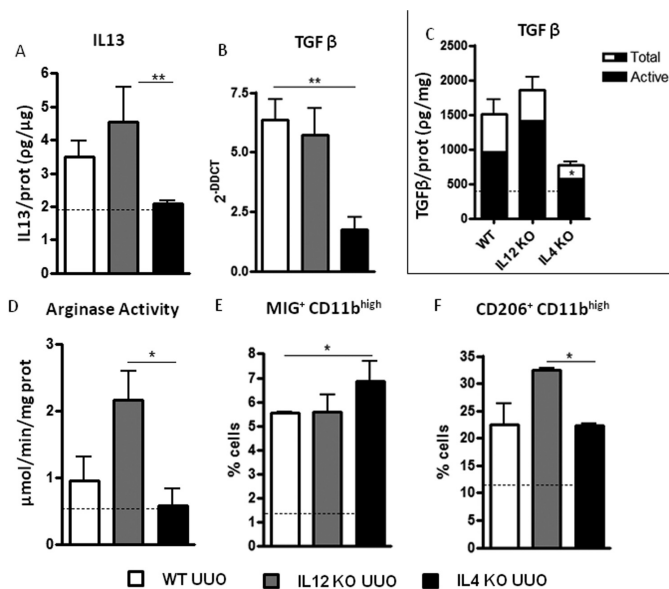


Figure 4. IL-4 deficiency impairs T_H2 and M2 immune response after UOU. IL-13 levels (A), TGF-β mRNA (B) and protein (C) expression and arginase-1 activity (D) in IL-4, IL-12 KO and WT mice submitted to UOU. Percentage of CD11b^{high} cells expressing CD206 (E) and MIG (F) in the kidney of mice subjected to UOU. qPCR was normalized to HPRT, and the mean of the WT control mice was considered 1. Dashed line represents WT animals not submitted to UOU. *p < 0.05, **p < 0.01.

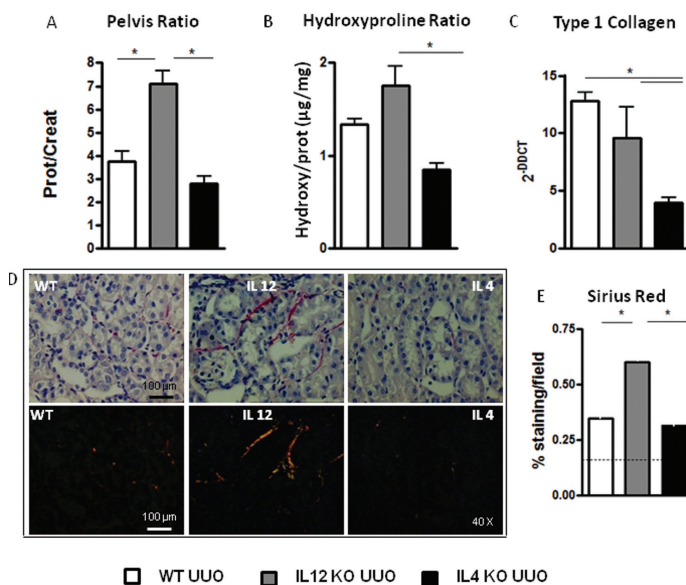


Figure 5. T_H2 immune response instigates the loss of renal function and increases the fibrosis development. Pelvis proteinuria:creatininuria (A) and hydroxyproline:protein (B) ratios in IL-4, IL-12 KO and WT animals 7 d after UOU. Type-1 collagen mRNA (C) and deposition (D and E) at 7 d after surgery in IL-4, IL-12 KO and WT animals. The Sirius red is represented by the proportion of the staining area to the total area of the field. qPCR was normalized to HPRT, and the mean of the WT control mice was considered 1. Dashed line represents WT animals not submitted to UOU. *p < 0.05. Scale bar, 100 μm.

animals showed a decreased percentage of CD11b^{high} and CD11b^{low} cells (Figures 3D, E). On the other hand, the percentage of CD11b^{high} cells expressing CCR7, an M1 marker, was increased in MyD88 KO animals (Figure 3F). CD11b^{high} cells expressing CD206 and IL-10, both M2 markers, were diminished in MyD88 KO, when compared with WT animals (Figures 3G, H). The percentage of CD11b^{high} cells expressing IL-12 (p40) and MIG was equal among all groups (Figures 3I, J). Altogether, these data suggested that TLR2, TLR4 and MyD88 KO mice are protected against fibrosis through impairment in mounting a T_H2 immune response and by favoring a M1 phenotype. This profile was more prominent in MyD88 KO animals.

Involvement of the T_H2-Driven Immune Response in Fibrosis

Our data suggest that a T_H2-biased immune response was associated with renal fibrosis. Thus, we investigated whether an impaired T_H2 immune condition would protect mice against UOU. First, we observed that IL-4 KO mice subjected to urine flow obstruction did not increase the production of IL-13 after UOU as WT and IL-12 KO mice did (Figure 4A). Our results also showed that IL-4 KO animals have diminished mRNA and protein TGF-β expression (Figures 4B, C). Furthermore, IL-4 KO mice showed decreased arginase-1 activity when compared with IL-12 KO mice (Figure 4D). Indeed, IL-4 KO animals showed increased infiltration of MIG⁺CD11b^{high} cells (Figure 4E), whereas IL-12 KO animals showed increased infiltration of CD206⁺CD11b^{high} cells in obstructed kidneys (Figure 4F). Despite physical damage caused by ureteral obstruction, IL-4 KO mice had decreased proteinuria (Figure 5A). IL-4-deficient mice also showed a decrease in hydroxyproline rate and in type 1 collagen mRNA (Figures 5B, C) when compared with controls. These data corroborated Sirius red staining analysis of renal tissue, where an increase in collagen deposition in IL-12 KO mice was significantly higher than those seen in IL-4 KO and WT mice (Figures 5D, E). Our

data confirmed the participation of the T_H2 -related cytokines in the development of fibrosis by different mechanisms.

Hematopoietic Source of T_H2 -Related Cytokine and Macrophages Are Responsible for Fibrosis Development

The microenvironment can modulate the immune response and thus interfere in macrophage and CD4 + T-cell activation. To determine whether the reduced fibrosis observed in obstructed IL-4 KO mice was due to IL-4 deficiency in parenchyma cells or in infiltrating leukocytes, we performed bone marrow (BM) chimera studies. Irradiated IL-12 KO mice were reconstituted with IL-4 KO BM, whereas irradiated IL-4 KO mice were reconstituted with IL-12 KO BM. As shown in Figure 6A, chimeric IL-12 to IL-4 KO animals had better renal outcomes, which were reflected by decreased proteinuria and a diminished fibrotic area (Figures 6B, C). In contrast, chimeric IL-4 to IL-12 KO animals had worse renal function.

To analyze the role of macrophages and T cells in development of renal fibrosis, we used clodronate liposomes to deplete macrophages (Supplementary Figure S2), and T-cell-deficient mice, respectively. Macrophages play a pivotal role in the development of tubular apoptosis and renal fibrosis (13,26). Clodronate administration led to better renal function (Figure 7A) and to a decreased renal fibrotic area (Figure 7B, C). In contrast, the absence of T cells did not change the proteinuria:creatininuria ratio or collagen deposition. These data confirm that macrophages influence fibrosis development in an UUO system.

DISCUSSION

Renal fibrosis is the result of an injury that leads to the production of ECM compounds. Because the obstruction is continuous, ECM deposition becomes massive, and the uncontrolled apoptosis of tubular cells results in tubular atrophy (4). This matrix remodeling and cellular stress release molecules that ultimately activate an inflammatory

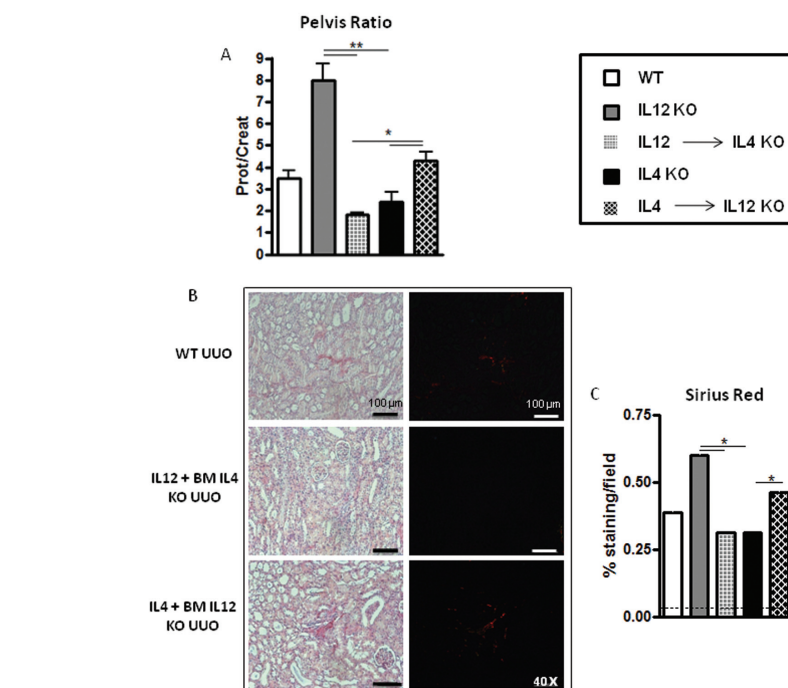


Figure 6. IL-4 and IL-12 BM chimera and renal fibrosis. Pelvis proteinuria:creatininuria ratio (A) in WT, KO nonchimeric and in KO chimeric animals. Collagen deposition quantification and staining (B and C) in chimeric animals. Dashed line represents WT animals not submitted to UUO. * $p < 0.05$, ** $p < 0.01$. Scale bar, 100 μ m.

response through innate sensing receptors. Some groups have demonstrated the importance of TLRs in chronic kidney injuries (5,7). TLR2, TLR4 and MyD88 are able to sense signals that ultimately lead to extracellular matrix deposition. We know TLR2 and TLR4-deficient animals present less fibrotic-associated process (4–6), however, it was unclear, until now, how the stimulation of such innate immune receptors can lead to fibrogenesis. Indeed, it has been proposed that T_H2 cytokines are implicated in fibrosis formation in lung and hepatic models of chronic diseases (10–12). Thus, we hypothesize that the signaling pathway of TLRs led to renal fibrosis development due to a polarization toward a T_H2 /M2-biased phenotype. Using an established experimental model of renal fibrosis, we observed that the absence of MyD88 signaling culminated in a decreased T_H2 /M2-related profile and protection against renal fibrosis formation.

We explored the role of MyD88-mediated innate immunity and the T_H2 /M2 immune deviated response, by investigating the T_H1 : T_H2 and M1:M2 balance in our model of disease. WT animals exhibited a T_H2 pattern following ureteral obstruction, whereas TLR2, TLR4 and MyD88 KO mice did not. In addition, we observed an increase in T_H1 -related cytokines in WT mice, but assumed that the increase in T_H2 -related cytokines had biological relevancy in a profibrotic environment. Additionally, the decreased levels of TGF- β , IL-13, IL-4, GATA-3, TSLP and arginase-1 activity observed in the deficient mice corroborated our hypothesis. IL-13, a T_H2 cytokine, promotes collagen production by distinct but overlapping mechanisms (27). IL-13 stimulates the production of latent TGF- β by macrophages, directly activates the collagen-producing machinery in fibroblasts and promotes the activation of alternative macrophages by upregulating arginase-1 activity (28). Members of the TGF- β su-

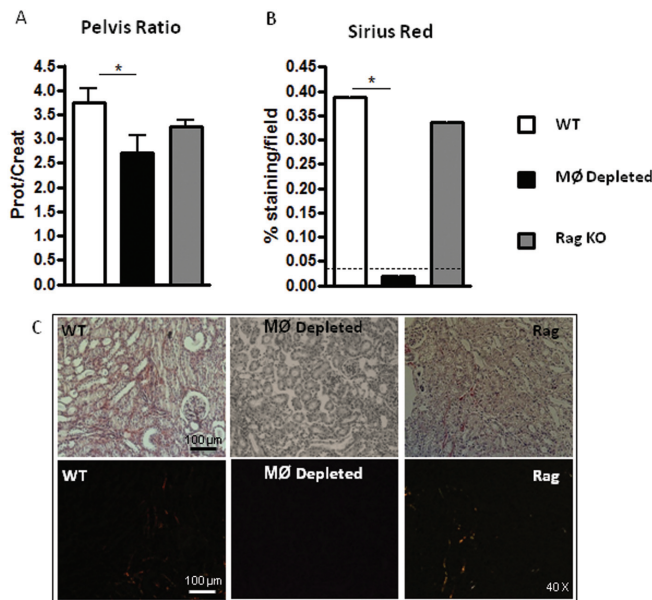


Figure 7. Macrophages influence renal fibrosis development. Pelvis proteinuria:creatininuria ratio (A) in macrophage-depleted WT, Rag-1 KO and WT animals submitted to UUO. Collagen deposition quantification and staining (B and C) in macrophage-depleted WT, Rag-1 KO and WT animals submitted to UUO. Dashed line represents WT animals not submitted to UUO. **p* < 0.05. MØ, macrophages. Scale bar, 100 µm.

perfamily are the most extensively studied macrophage-derived growth factors that have been linked to renal fibrosis. This cytokine is a potent chemoattractant for macrophage/monocyte cells and can induce myofibroblast transformation via epithelial- or endothelial-to-mesenchymal transitions (29). In our model, the expression of IL-13 and TGF-β was present in all mice with increased collagen deposition. Finally, TSLP, which was reduced in TLR2-, TLR4- and MyD88-deficient animals, is described as effective for the differentiation of CD4⁺ T_H2 cells. The combination of TCR stimulation and TSLP signaling induce IL-4 transcription and further T_H2 polarization (30). Therefore, the decreased levels of these T_H2-related products observed in protected mice leads to the conclusion that ureteral obstruction induces fibrosis development in a manner dependent on the T_H2 immune response.

Finally, to determine the source of the T_H2-related cells, we investigated the contribution of infiltrating hematopoietic and/or resident parenchymal cells in fi-

brosis formation. We performed chimeric experiments and observed that recipient IL-12 KO animals from IL-4 bone marrow KO mice demonstrated better renal function and decreased collagen deposition, which suggests a dependency of IL-4 from hematopoietic cells to generate fibrosis. T lymphocytes and macrophages are included in such hematopoietic cells, but the role of T lymphocytes in fibrosis formation is controversial. Tapmeier *et al.* stated CD4⁺ T cells have a pivotal role in ureteric obstruction (31). However, this group found no difference in tubular damage, in the number of F4/80⁺ macrophages and TGF-β mRNA expression when comparing Rag-1 KO and WT mice, which leads us to argue that the reduction in Masson trichrome in Rag-1 KO mice could be the result of a less profibrotic phenotype in the macrophage infiltrate. Otherwise, Shappell *et al.* demonstrated that the absence of T cells does not change the tubular atrophy and interstitial volume expansion when compared with mice with T cells in a model of obstructive nephropathy (32). Our

data corroborate Shappell's study, indicating the fibrotic response is an indirect consequence of T cell-mediated renal injury, rather than T cells being directly involved in fibrosis. It seems T cells influence macrophage function and collagen deposition by fibroblasts.

Macrophage infiltration of the kidney is a prominent feature associated with the severity of renal injury and progressive renal failure (15). Several groups have shown that systemic depletion of phagocytes with liposomal clodronate in different immune-mediated renal injury models reduces morphologic kidney damage (26,27,33). However, recent studies raise the possibility that the effector phenotype of the recruited macrophages, rather than their presence, determines the extent of renal parenchymal injury (34,35). Wang and colleagues demonstrated that M1 infusion leads to worse kidney parameters in a proinflammatory model of renal disease (15). The presence of proinflammatory macrophages in injured organs has been shown to increase the generation of reactive oxygen species (ROS) and to induce the death of injured tubular cells (36). Additionally, the population of M2 macrophages increases when cell proliferation occurs, mainly in chronic models of injured kidney. Lee *et al.* demonstrated that M1 macrophages decrease iNOS expression and increase M2 markers in contact with proximal tubule cells either in an *in vitro* system or with the injury becoming chronic *in vivo* (34). However, more studies must be conducted to clarify to what extent different macrophage subpopulations are attracted to the kidney or to what extent a single cell is able to cause damage or to regulate the scar process. Based on the wound healing process, Anders *et al.* proposed four different types of macrophages: M1 macrophages induced by renal infection and cell necrosis; M2c/suppressor macrophages induced by uptake of apoptotic cells; M2a/wound healing macrophages induced by abundant growth factor secretion; and fibrolytic macrophages, able to solve the scar process (37). In the present study, we investi-

gated the presence of M1 and M2a macrophages, and we found a decreased number of M2a macrophages in TLR2, TLR4, MyD88 and IL-4 KO mice that, ultimately, presented less fibrosis.

CONCLUSION

Therefore, we propose that a urinary obstruction flow model generates the recruitment and the activation of M2 macrophages as well as the stimulation of a T_H2 immune response, in a MyD88-dependent manner. This process culminates in extracellular matrix deposition and fibrosis formation (Supplementary Figure S3). Taken together, these results provide evidence that future therapeutic strategies against renal fibrosis should be accompanied by the modulation of the M1:M2 and $T_H1:T_H2$ balance and this control appears to be essential in chronic kidney disease, making T_H2 and M2 cells predictive of fibrosis.

ACKNOWLEDGMENTS

This work was supported by the Brazilian Foundation – FAPESP (Fundação de Apoio à Pesquisa do Estado de São Paulo), Grant Numbers: 07/07139-3 and 10/52180-4), International Associated Laboratory (CNPq/Inserm) and National Institute of Science and Technology (INCT) Complex Fluids. The authors thank Bernardo Paulo Albe for preparing the histology slides and Cláudia Silva Cunha for technical assistance.

DISCLOSURE

The authors declare that they have no competing interests as defined by *Molecular Medicine*, or other interests that might be perceived to influence the results and discussion reported in this paper.

REFERENCES

- Mangione F, Dal Canton A. (2010) The epidemic of chronic kidney disease: looking at ageing and cardiovascular disease through kidney-shaped lenses. *J. Intern. Med.* 268:449–55.
- Nagle RB, Bulger RE, Cutler RE, Jervis HR, Benditt EP. (1973) Unilateral obstructive nephropathy in the rabbit. I. Early morphologic, physiologic, and histochemical changes. *Lab. Invest.* 28:456–7.
- Bascands JL, Schanstra JP. (2005) Obstructive nephropathy: insights from genetically engineered animals. *Kidney Int.* 68:925–37.
- Pulsikens WP, et al. (2010) TLR4 promotes fibrosis but attenuates tubular damage in progressive renal injury. *J. Am. Soc. Nephrol.* 21:1299–308.
- Pradere JP, Troeger JS, Dapito DH, Mencin AA, Schwabe RF. (2010) Toll-like receptor 4 and hepatic fibrogenesis. *Semin. Liver Dis.* 30:232–44.
- Leemans JC, et al. (2009) The role of Toll-like receptor 2 in inflammation and fibrosis during progressive renal injury. *PLoS One.* 4:e5704.
- Skuginna, et al. (2011) Toll-like receptor signaling and SIGIRR in renal fibrosis upon unilateral ureteral obstruction. *PLoS One.* 6:e19204.
- Martinon F, Petrilli V, Mayor A, Tardivel A, Tschopp J. (2006) Gout-associated uric acid crystals activate the NALP3 inflammasome. *Nature.* 440:237–41.
- Kool M, et al. (2011) An unexpected role for uric acid as an inducer of T helper 2 cell immunity to inhaled antigens and inflammatory mediator of allergic asthma. *Immunity.* 34:527–40.
- Cheever AW, et al. (1994) Anti-IL-4 treatment of *Schistosoma mansoni*-infected mice inhibits development of T cells and non-B, non-T cells expressing Th2 cytokines while decreasing egg-induced hepatic fibrosis. *J. Immunol.* 153:753–9.
- Chiaromonte MG, Donaldson DD, Cheever AW, Wynn TA. (1999) An IL-13 inhibitor blocks the development of hepatic fibrosis during a T-helper type 2-dominated inflammatory response. *J. Clin. Invest.* 104:777–85.
- Reiman RM, et al. (2006) Interleukin-5 (IL-5) augments the progression of liver fibrosis by regulating IL-13 activity. *Infect. Immun.* 74:1471–9.
- Sung SA, Jo SK, Cho WY, Won NH, Kim HK. (2007) Reduction of renal fibrosis as a result of liposome encapsulated clodronate induced macrophage depletion after unilateral ureteral obstruction in rats. *Nephron. Exp. Nephrol.* 105:e1–9.
- Kitamoto K, et al. (2009) Effects of liposome clodronate on renal leukocyte populations and renal fibrosis in murine obstructive nephropathy. *J. Pharmacol. Sci.* 111:285–92.
- Wang Y, et al. (2007) Ex vivo programmed macrophages ameliorate experimental chronic inflammatory renal disease. *Kidney Int.* 72:290–9.
- Vinuesa E, et al. (2008) Macrophage involvement in the kidney repair phase after ischaemia/reperfusion injury. *J. Pathol.* 214:104–13.
- Mosser DM, Edwards JP. (2008) Exploring the full spectrum of macrophage activation. *Nat. Rev. Immunol.* 8:958–69.
- Loke P, et al. (2007) Alternative activation is an innate response to injury that requires CD4+ T cells to be sustained during chronic infection. *J. Immunol.* 179:3926–36.
- Brandt E, Woerly G, Younes AB, Loiseau S, Capron M. (2000) IL-4 production by human polymorphonuclear neutrophils. *J. Leukoc. Biol.* 68:125–30.
- Wilson MS, Wynn TA. (2009) Pulmonary fibrosis: pathogenesis, etiology and regulation. *Mucosal Immunol.* 2:103–21.
- Reddy GK, Enwemeka CS. (1996) A simplified method for the analysis of hydroxyproline in biological tissues. *Clin. Biochem.* 29:225–9.
- Deamer D, Bangham AD. (1976) Large volume liposomes by an ether vaporization method. *Biochim. Biophys. Acta.* 443:629–34.
- Tsuboi N, et al. (2002) Roles of toll-like receptors in C-C chemokine production by renal tubular epithelial cells. *J. Immunol.* 169:2026–33.
- Edgton KL, Gow RM, Kelly DJ, Carmeliet P, Kitching AR. (2004) Plasmin is not protective in experimental renal interstitial fibrosis. *Kidney Int.* 66:68–76.
- Tan AM, et al. (2010) TLR4 signaling in stromal cells is critical for the initiation of allergic Th2 responses to inhaled antigen. *J. Immunol.* 184:3535–44.
- Sung SA, Jo SK, Cho WY, Won NH, Kim HK. (2007) Reduction of renal fibrosis as a result of liposome encapsulated clodronate induced macrophage depletion after unilateral ureteral obstruction in rats. *Nephron. Exp. Nephrol.* 105:e1–9.
- Kitamoto K et al. (2009) Effects of liposome clodronate on renal leukocyte populations and renal fibrosis in murine obstructive nephropathy. *J. Pharmacol. Sci.* 111:285–92.
- Wynn TA. (2003) IL-13 effector functions. *Annu. Rev. Immunol.* 21:425–56.
- Lee SB, Kalluri R. (2010) Mechanistic connection between inflammation and fibrosis. *Kidney Int. Suppl.*S22–26.
- Ziegler SF, Artis D. (2010) Sensing the outside world: TSLP regulates barrier immunity. *Nat. Immunol.* 11:289–93.
- Tapmeier TT, et al. (2010) Pivotal role of CD4+ T cells in renal fibrosis following ureteric obstruction. *Kidney Int.* 78:351–62.
- Shappell SB, Gurpinar T, Lechago J, Suki WN, Truong LD. (1998) Chronic obstructive uropathy in severe combined immunodeficient (SCID) mice: lymphocyte infiltration is not required for progressive tubulointerstitial injury. *J. Am. Soc. Nephrol.* 9:1008–17.
- Jo SK, Sung SA, Cho WY, Go KJ, Kim HK. (2006) Macrophages contribute to the initiation of ischaemic acute renal failure in rats. *Nephrol. Dial. Transplant.* 21:1231–9.
- Lee S, et al. (2011) Distinct macrophage phenotypes contribute to kidney injury and repair. *J. Am. Soc. Nephrol.* 22:317–26.
- Patschan D, Patschan S, Gobe GG, Chintala S, Goligorsky MS. (2007) Uric acid heralds ischemic tissue injury to mobilize endothelial progenitor cells. *J. Am. Soc. Nephrol.* 18:1516–24.
- Pazar B, et al. (2011) Basic calcium phosphate crystals induce monocyte/macrophage IL-1 β secretion through the NLRP3 inflammasome in vitro. *J. Immunol.* 186:2495–502.
- Anders JH, Ryu M. (2011) Renal microenvironments and macrophage phenotypes determine progression or resolution of renal inflammation and fibrosis. *Kidney Int.* 9:915–25.